

Neutrino Counter Nuclear Weapon

Alfred Tang*

(Dated: October 25, 2018)

Radiations produced by neutrino-antineutrino annihilation at the Z^0 pole can be used to heat up the primary stage of a thermonuclear warhead and can in principle detonate the device remotely. Neutrino-antineutrino annihilation can also be used as a tactical assault weapon to target hideouts that are unreachable by conventional means.

I. INTRODUCTION

Nuclear weapon is the most destructive kind among weapons of mass destruction. Hiroshima and Nagasaki are lessons in history that shall never be repeated. Since the end of World War II, world leaders had tried to control the proliferation of nuclear weapons by political means such as the Nuclear Non-proliferation Treaty in 1968. Many countries did not sign the treaty. In fact it seems that more and more countries are pursuing nuclear weapon programs nowadays. After September 11, the concern is that nuclear weapons will fall into the hands of terrorists. Strategically speaking the importance of a counter nuclear weapon may soon rival that of the nuclear weapon itself. The purpose of this paper is to explore the possibility of a neutrino counter nuclear weapon technology. The idea of using neutrinos to detonate or melt a nuclear weapon was first proposed by H. Sugawara, H. Hagura and T. Sanami [1]. Their futuristic design is based on a 1 PeV neutrino beam operating at 50 GW. It is unlikely that such an intense ultra high energy neutrino beam can be realized in the near future. Even if such a neutrino beam is made available, its radiation hazard will render it politically nonviable. Other proposals such as installing neutron detectors at the border to intercept nuclear materials had been considered. The current trend of non-proliferation policy is focused on monitoring the production of fissile fuels. Research is being conducted to use anti-neutrino detectors to this end [2]. Anti-neutrinos are produced in nuclear fission through beta decay. They are indicators of the fissile fuel composition of the nuclear reactor. Neutrino signatures of the fissile fuels cannot be tampered with by virtue of the very small reaction cross section of neutrinos at low energy. On the other hand, the small reaction probability also means small detection probability so that large detectors are needed to detect them. A sample idea is to deploy hundreds of kilo-ton liquid scintillator detectors at 1000 km distance from the reactor to monitor the reactor anti-neutrino spectrum. The challenges of using anti-neutrino to monitor reactor are that (1) a rogue nation will not voluntarily allow IAEA to build anti-neutrino detectors around its reactors, (2) the number of anti-neutrino detectors must increase 4 folds for every doubling of reactor-detector distance, and (3) reactors are not needed if a rogue nation opts for uranium instead of plutonium bombs. For these reasons, anti-neutrino detectors are probably not the ultimate solution to non-proliferation. Another possible non-proliferation strategy is to develop a technology that counters nuclear weapons.

This paper proposes an alternative idea for a neutrino counter nuclear weapon that shares some similarities with the idea presented in Reference [1] but is technologically feasible, relatively cheap and safe. The present idea is to focus a neutrino beam and an antineutrino beam together in a small region to allow them to annihilate so that high energy radiations are released as reaction products. The radiations cause neutron spallation in the sub-critical nuclear material and initiate fission reactions. The plutonium heats up, ignites the chemical explosive around the fissile (fissionable material) in the primary stage of a thermonuclear warhead and subsequently detonates the nuclear weapon. The reason of thinking about neutrino for this application is that neutrino cannot be shielded. It can hit a target such as a nuclear submarine from the other side of the globe and can penetrate a deep underground concrete bunker and missile silo. Since neutrino can penetrate the planet to reach a nuclear weapon on the other side of the globe near the speed of light, a neutrino counter nuclear weapon is in principle untraceable and indefensible. It is suggested that a neutrino counter nuclear weapon is 100% effective [3].

The trade-off of developing a counter weapon is the introduction of a new weapon. If the new weapon is less destructive than the original weapon, an ethical argument can be made in support of its development. If remote detonation of a nuclear weapon is made possible by a neutrino counter weapon, a nuclear weapon in the homeland becomes a liability so that there is a real strategic incentive to reduce the stockpile. In that case, there will be a much more convincing political reason to promote non-proliferation. This work aims to study the theoretical feasibility of the neutrino counter nuclear weapon as a first step in this direction. The use of neutrino as a tactical assault weapon

*Electronic address: atang@fnal.gov

will also be discussed.

II. THEORETICAL PREPARATION

One of the properties of neutrino is that it has a vanishingly small interaction cross section so that it is the most penetrative radiation known to be in existence today. The invariant amplitude \mathcal{M} is proportional to the weak boson (massive spin-1) propagator [4–6]

$$\frac{-i(g_{\mu\nu} - q_\mu q_\nu/M^2)}{q^2 - M^2 + i\epsilon}, \quad (1)$$

where q is the transfer momentum, M is the weak boson mass and the infinitesimal ϵ moves the pole away from the branch so that Eq. (1) is mathematically well defined. The weak bosons are W^\pm and Z^0 . The corresponding masses are $M_W = 80.403 \pm 0.029$ GeV and $M_Z = 91.1876 \pm 0.0021$ GeV [7]. In the case of an unstable particle with a total decay width Γ , it is customary to make the replacement $M^2 \rightarrow M^2 + iM\Gamma$ according to the Breit-Wigner resonance formula so that Eq. (1) becomes [8]

$$\frac{-i(g_{\mu\nu} - q_\mu q_\nu/M^2)}{q^2 - M^2 - iM\Gamma}. \quad (2)$$

It is said that the propagator in Eq. (2) violates gauge invariance and that slightly more elaborate modifications are needed [9, 10]. It is also suggested that Eq. (2) is not theoretically justified in quantum mechanics and quantum field theory and is motivated mostly by phenomenology [11]. Eq. (2) also violates Lorentz invariance in a subtle way. The decay width Γ is typically measured in the rest frame of the particle and is related to the lifetime of the particle τ_0 in its rest frame as $\tau_0 = 1/\Gamma$. Lifetime is not Lorentz invariant and can be dilated ($\tau = \gamma\tau_0$). Traditionally Γ in Eq. (2) is taken to be a constant just like M . As it will be shown later, the width term can be eliminated from the final result by special relativistic considerations. For the sake of simplicity, only Eq. (1) with $\epsilon = 0$ will be used in the calculations of the invariant amplitude \mathcal{M} in this section. When $q^2 \ll M^2$, the propagator in Eq. (1) is reduced to $ig_{\mu\nu}/M^2$ and is weighted down by a very heavy weak boson mass such that the invariant amplitude becomes very small. It is the reason why neutrino is so non-interactive even though the weak coupling constants g_W and g_Z are both larger than the electromagnetic coupling constant g_e [4],

$$g_W = \frac{g_e}{\sin \theta_w}, \quad (3)$$

$$g_Z = \frac{g_e}{\sin \theta_w \cos \theta_w}, \quad (4)$$

$$G_F = \frac{\sqrt{2}}{8} \left(\frac{g_W}{M_W} \right)^2, \quad (5)$$

where $g_e = 7.297352568 \times 10^{-3}$, θ_w is the Weinberg angle ($\sin^2 \theta_w = 0.23122$) and G_F is the Fermi constant ($G_F = 1.16637 \times 10^{-5}$ GeV⁻²) [7]. As a corollary, large M_W is the reason why the inverse beta decay cross section is vanishingly small. The present work focuses only on the tree-level diagrams such as $\nu\bar{\nu} \rightarrow l\bar{l}$ and $\nu\bar{\nu} \rightarrow f\bar{f}$ (l for “lepton”, f for “fermion”) as shown in Fig. 1. Reactions such as $\nu\bar{\nu} \rightarrow \gamma\gamma$ is possible but is a higher-order diagram [12]. It turns out that a W^\pm pole is impossible for a charged current in the Feynman diagram of Figure 1a because the transfer momentum is always null ($q^2 = 0$) or spacelike ($q^2 < 0$) as it will be shown later. In the case of neutral current in Figure 1b, the transfer momentum can be timelike ($q^2 > 0$) so that a Z^0 pole is possible at $q^2 = M_Z^2$. The Z^0 pole has been experimentally observed in the spectrum of e^+e^- scattering at LEP and SLAC since 1989 [6] and in $p\bar{p}$ scattering experiments at Fermilab [13]. This work takes advantage of the Z^0 pole to maximize the neutrino-antineutrino annihilation cross section to produce high energy radiation in a maximally efficient way.

For the charged current in Figure 1a, The flavor of the outgoing lepton l (antilepton \bar{l}) must match that of the incoming ν ($\bar{\nu}$) at each vertex. Mixed flavors are possible in a reaction as a whole. For example, $\nu_e\bar{\nu}_\mu \rightarrow e^-e^+$, $\nu_e\bar{\nu}_\mu \rightarrow e^-\mu^+$ and all other combinations are allowed. The invariant amplitude of $\nu\bar{\nu} \rightarrow l\bar{l}$ in Fig. 1a is

$$\begin{aligned} \mathcal{M}_W &= -\frac{g_W^2}{8(q^2 - M_W^2)} [\bar{u}_\nu \gamma^\mu (1 - \gamma^5) u_l] \left(g_{\mu\nu} - \frac{q_\mu q_\nu}{M_W^2} \right) [\bar{v}_l \gamma^\nu (1 - \gamma^5) v_\nu] \\ &\simeq -\frac{g_W^2}{8(q^2 - M_W^2)} [\bar{u}_\nu \gamma^\mu (1 - \gamma^5) u_l] [\bar{v}_l \gamma_\mu (1 - \gamma^5) v_\nu]. \end{aligned} \quad (6)$$

The transfer momentum is $q = p_l - p_\nu = p_{\bar{\nu}} - p_{\bar{l}}$. The approximations made in the second step of Eq. (6) are the small masses of neutrino ($m_\nu \sim 0$) and lepton ($m_l \ll M_W$). The invariant amplitude is squared, summed over final spins and averaged over initial spins. This calculation is simplified by applying the usual Casimir's trick and trace theorems. Neutrino has helicity $h = -1$ but antineutrino has $h = +1$ so that there is only 1 spin state for each initial neutrino or antineutrino. The Casimir trick sums over all initial and final spin states by default. By "averaging over initial spins", it simply means that the sum must be divided by the proper factor to avoid over-counting. This way the sum over initial spins must be divided by 2 for each initial neutrino or antineutrino. For a reaction involving 2 incoming neutrinos, the proper invariant amplitude square $\langle \mathcal{M}^2 \rangle$ needs to be divided by 4. With the standard procedure outlined above, Eq. (6) can be squared, summed and averaged to give

$$\langle \mathcal{M}_W^2 \rangle = \left[\frac{g_W^2}{q^2 - M_W^2} \right]^2 (p_l \cdot p_{\bar{\nu}})(p_\nu \cdot p_{\bar{l}}). \quad (7)$$

Since the present calculation is focused on high energy ($q^2 \rightarrow M^2$), the rest mass of neutrino and lepton can be neglected ($m_\nu \rightarrow 0$ and $m_l \rightarrow 0$). In the lab frame, the 4-momenta can be parametrized as $p = (E, p_x, p_y, p_z)$ in such a way that 4-momentum is conserved by definition:

$$p_1 \simeq E_1(1, \sin \theta_1, 0, \cos \theta_1), \quad (8)$$

$$p_2 \simeq E_2(1, -\sin \theta_2, 0, \cos \theta_2), \quad (9)$$

$$p_3 \simeq E_3(1, \sin \theta \cos \phi, \sin \theta \sin \phi, \cos \theta), \quad (10)$$

$$p_4 \simeq p_1 + p_2 - p_3. \quad (11)$$

The z -axis in Eqs. (8)–(11) is chosen to point in the direction of the sum of the initial 3-momenta $\mathbf{p}_1 + \mathbf{p}_2$. The outgoing 3-momenta \mathbf{p}_3 and \mathbf{p}_4 can rigidly rotate around the z -axis through the azimuthal angle ϕ and still conserve 3-momentum. For the sake of illustration, Fig. 2 shows a special case in that all of the incoming and outgoing 3-momenta lie on the same plain. The distance between the foci \mathcal{F} and \mathcal{F}' corresponds to the vectorial sum $\mathbf{p}_1 + \mathbf{p}_2 = \mathbf{p}_3 + \mathbf{p}_4$ so that 3-momentum is conserved automatically. Assuming the high energy condition $E_i \gg m_i$, $E_i \simeq |\mathbf{p}_i|$ for $i \in \{1, 2, 3, 4\}$. The ellipsoid \mathcal{E} constrains the point \mathcal{O} in such a way that $|\mathbf{p}_1| + |\mathbf{p}_2| = |\mathbf{p}_3| + |\mathbf{p}_4|$ so that energy is conserved by $E_1 + E_2 = E_3 + E_4$. In essence, the construction in Fig. 2 guarantees the conservation of 4-momentum as long as the high energy condition is met. In the special case of $\theta_1 \rightarrow 0$ and $\theta_2 \rightarrow 0$, the approximations $E_i \simeq |\mathbf{p}_i|$ made in Eqs. (8)–(11) may become invalid and should be replaced by the exact parametrizations

$$p_i = (E_i, |\mathbf{p}|_i \sin \theta_i \cos \phi_i, |\mathbf{p}|_i \sin \theta_i \sin \phi_i, |\mathbf{p}|_i \cos \theta_i). \quad (12)$$

However small values of θ_1 and θ_2 do not have any practical advantage and will not be used in this work. For the charged current diagram of Fig. 1a, $p_1 = p_\nu$, $p_2 = p_{\bar{\nu}}$, $p_3 = p_l$ and $p_4 = p_{\bar{l}}$.

The azimuthal angle ϕ is not constrained by kinematics and is completely random. The transfer momentum square q^2 in the charged current diagram of Fig. 1a can be expressed in terms of the parametrizations in Eqs. (8)–(11) as

$$q^2 = (p_l - p_\nu)^2 \simeq -2E_\nu E_l (1 - \sin \theta_1 \sin \theta \cos \phi - \cos \theta_1 \cos \theta). \quad (13)$$

Regardless of the value of ϕ , the right-hand side of Eq. (13) is always non-positive. Therefore q^2 in $\langle \mathcal{M}_W^2 \rangle$ of Eq. (7) is either null ($q^2 = 0$) or spacelike ($q^2 < 0$). A W^\pm pole is impossible in principle in the charged current case because it is always true that $q^2 \neq M_W^2$.

The invariant amplitude for the neutral current diagram in Fig. 1b is

$$\begin{aligned} \mathcal{M}_Z &= -\frac{g_Z^2}{8(q^2 - M_Z^2)} [\bar{v}_{\bar{\nu}} \gamma^\mu (1 - \gamma^5) u_\nu] \left(g_{\mu\nu} - \frac{q_\mu q_\nu}{M_Z^2} \right) [\bar{u}_f \gamma^\nu (C_V - C_A \gamma^5) v_{\bar{f}}] \\ &\simeq -\frac{g_Z^2}{8(q^2 - M_Z^2)} [\bar{v}_{\bar{\nu}} \gamma^\mu (1 - \gamma^5) u_\nu] [\bar{u}_f \gamma_\mu (C_V - C_A \gamma^5) v_{\bar{f}}]. \end{aligned} \quad (14)$$

The flavor of $\nu\bar{\nu}$ cannot mix. The type of $f\bar{f}$ can vary but the flavor cannot mix. The values of the neutral vector coupling C_V and axial-vector coupling C_A are given by the GWS (Glashow-Weinberg-Salam) Model and are tabulated in Table I. Applying the usual rules, the invariant amplitude square can be computed as

$$\langle \mathcal{M}_Z^2 \rangle = \frac{1}{4} \left[\frac{g_Z^2}{q^2 - M_Z^2} \right]^2 \{ (C_V^2 + C_A^2) [(p_{\bar{\nu}} \cdot p_f)^2 + (p_\nu \cdot p_{\bar{f}})^2] + 2C_A C_V [(p_{\bar{\nu}} \cdot p_f)^2 - (p_\nu \cdot p_{\bar{f}})^2] \}. \quad (15)$$

The parametrizations in Eqs. (8)–(11) can be re-applied with the substitutions $p_1 = p_\nu$, $p_2 = p_{\bar{\nu}}$, $p_3 = p_f$ and $p_4 = p_{\bar{f}}$. The transfer momentum square in the neutral current case is

$$q^2 = (p_\nu + p_{\bar{\nu}})^2 \simeq 2(p_\nu \cdot p_{\bar{\nu}}) = 2E_\nu E_{\bar{\nu}} [1 - \cos(\theta_1 + \theta_2)]. \quad (16)$$

According to Fig. 1b, $0 \leq \theta_i \leq \pi/2$ for $i \in \{1, 2\}$ so that $q^2 \geq 0$ in Eq. (16). Therefore a Z^0 pole is possible for $\langle \mathcal{M}_Z^2 \rangle$ in Eq. (15) at $q^2 = M_Z^2$. On the average, $\langle \cos \phi \rangle = 0$ and $\langle \cos^2 \phi \rangle = 1/2$. The remaining kinematic factors in $\langle \mathcal{M}_Z^2 \rangle$ of Eq. (15) can be calculated as

$$(p_\nu \cdot p_f)^2 = E_\nu^2 E_f^2 \left(1 - 2 \cos \theta_1 \cos \theta + \frac{1}{2} \sin^2 \theta_1 \sin^2 \theta + \cos^2 \theta_1 \cos^2 \theta \right), \quad (17)$$

$$(p_{\bar{\nu}} \cdot p_f)^2 = E_{\bar{\nu}}^2 E_f^2 \left(1 - 2 \cos \theta_2 \cos \theta + \frac{1}{2} \sin^2 \theta_2 \sin^2 \theta + \cos^2 \theta_2 \cos^2 \theta \right). \quad (18)$$

Letting $E_\nu = E_{\bar{\nu}}$ leads to $\theta_1 = \theta_2$ which in turn gives $(p_\nu \cdot p_f)^2 = (p_{\bar{\nu}} \cdot p_f)^2$ so that the form of Eq. (15) is greatly simplified. Letting $E_\nu = E_{\bar{\nu}}$ has an additional advantage that the intensities of ν_e , ν_μ and ν_τ in the neutrino beam will match those of $\bar{\nu}_e$, $\bar{\nu}_\mu$ and $\bar{\nu}_\tau$ in the antineutrino beam despite of neutrino oscillation as long as the original neutrino-antineutrino beams have the same intensities and the matter effect of the earth is either negligible or canceled by symmetry.

The cross section formula of the reaction $1 + 2 \rightarrow 3 + 4 + \dots + n$ can be calculated by the Fermi's Golden Rule [4],

$$d\sigma = \langle \mathcal{M}^2 \rangle \frac{S}{4\sqrt{(p_1 \cdot p_2)^2 - (m_1 m_2)^2}} \left[\left(\frac{d^3 \mathbf{p}_3}{(2\pi)^3 2E_3} \right) \left(\frac{d^3 \mathbf{p}_4}{(2\pi)^3 2E_4} \right) \dots \left(\frac{d^3 \mathbf{p}_n}{(2\pi)^3 2E_n} \right) \right] \times (2\pi)^4 \delta^4(p_1 + p_2 - p_3 - p_4 - \dots - p_n), \quad (19)$$

where S is a statistical factor that includes a factor of $1/j$ for each type of j identical outgoing particles. For the Feynman diagrams in Fig. 1, $S = 1$ and $n = 4$. The differential cross section for the neutral current diagram can be obtained from Eq. (19) after performing integrations over \mathbf{p}_3 and \mathbf{p}_4 ,

$$\frac{d\sigma}{d\Omega} = \frac{1}{(8\pi)^2} \frac{\langle \mathcal{M}_Z^2 \rangle}{E_\nu E_{\bar{\nu}} [1 - \cos(\theta_1 + \theta_2)]} \times \frac{E_f}{E_\nu + E_{\bar{\nu}} - \cos \theta \sqrt{(E_\nu \sin \theta_1 - E_{\bar{\nu}} \sin \theta_2)^2 + (E_\nu \cos \theta_1 + E_{\bar{\nu}} \cos \theta_2)^2}}. \quad (20)$$

Eq. (20) is useful for checking pathology in the theory. In this case, there is no pathology related to the cross section formula. It is checked that $d\sigma/d\Omega \propto \langle \mathcal{M}_Z^2 \rangle$. Although the exact form of the cross section formula is unimportant for the the purpose of this work, Eq. (20) is useful for calculating the relative distributions of the outgoing particles once the infinity of $1/[q^2 - M_Z^2]$ at the Z^0 pole is canceled out by division. At the Z^0 pole, the cross section in Eq. (20) is infinite and the interaction probability is 1. This way, the flux of annihilation-induced radiations is directly proportional to the intensities of the $\nu\bar{\nu}$ beams. For the purpose of designing an efficient neutrino weapon, Eq. (16) used in $q^2 = M_Z^2$ is the key result of this section. The branching ratios of various annihilation-induced products $f\bar{f}$ can be calculated by comparing $\langle \mathcal{M}_Z^2 \rangle$ using Eq. (15). In the case $E_\nu = E_{\bar{\nu}}$, the branching ratios are particularly simple and can be obtained from ratios of $C_V^2 + C_A^2$ alone.

Finally the earlier claim that the width term $iM\Gamma$ can be eliminated from the final result by special relativity needs to be explained. Historically the width is incorporated in the scattering amplitude $f(E)$ in non-relativistic quantum mechanics as in [8, 14]

$$f(E) \propto \frac{1}{E - E_0 + i\Gamma/2}. \quad (21)$$

It is observed in low energy inelastic scattering experiments that an incoming particle form a compound nucleus with the nucleons of the target nucleus as an intermediate state. The discrete energy levels E_0 of this compound nucleus give rise to resonances. If the compound nucleus is unstable, the resonance is modified as $E_0 \rightarrow E_0 - i\Gamma/2$. It is the so-called Breit-Wigner resonance. In experiments, E_0 and Γ are extracted from partial wave analysis. In hadron physics, Γ is modeled as a function of energy $\Gamma \rightarrow \Gamma(W)$, where W is the energy in the center-of-momentum (CM) frame, along with other model dependent parameters [15]. With minor adjustments, the Breit-Wigner formula is phenomenologically robust. Sometimes there are disagreements among different analyses on some of the parameters. An example is the E_{0+} parameter in the cross section of the η photoproduction of $S_{11}(1535)$ [16–19]. In this case,

the discrepancy is thought to have come from different experimental biases and the difficulties in resolving nearby resonances. So far the validity of Eq. (21) is not questioned. Although the form of Eq. (21) has been discussed in many quantum mechanics textbooks [14], the $iM\Gamma$ term in the propagator of Eq. (2) in quantum field theory is not derived from first principle but is borrowed from quantum mechanics. Reference [8] contains a heuristic explanation of Eq. (2) as

$$\frac{1}{p^2 - M^2 + iM\Gamma} \approx \frac{1}{2E_{\mathbf{p}}(p^0 - E_{\mathbf{p}} + i(M/E_{\mathbf{p}})\Gamma/2)}. \quad (22)$$

In Eq. (22), p^0 is the pole and $E_{\mathbf{p}}$ is the energy of the particle. The factor $M/E_{\mathbf{p}}$ is the reciprocal of the Lorentz factor $1/\gamma$ that accounts for the relativistic correction of the lifetime of the particle $\tau = \gamma\tau_0$. The right-hand side of Eq. (22) is a combination of Eq. (21) with the replacement $\Gamma \rightarrow \Gamma/\gamma$ and a factor of $1/2E_{\mathbf{p}}$ that commonly appears in relativistic quantum mechanics and quantum field theory. Since the relativistic effect is already included by virtue of incorporating $1/\gamma$ on the right-hand side of Eq. (22), Γ on the left-hand side can be taken as a constant much like the rest mass M is a constant. The implicit Lorentz factor γ on the right hand side of Eq. (22) is frame dependent. The left hand side is manifestly frame independent. This ambiguity is a proof that Eq. (22) is not a theory but a phenomenological patch. Since Eq. (22) is borrowed from Eq. (21), it is reasonable to assume that the validity of the former is based on the satisfaction of the same conditions of the latter. The basic assumptions of Eq. (21) are the target nucleus and compound nucleus at rest in the lab frame and a total width Γ measured in the same rest frame. In high energy scattering experiments such as $e^+e^- \rightarrow Z^0$ and $p\bar{p} \rightarrow Z^0$, the equivalent of a target nucleus can be taken to be the center-of-mass of the in-state. So far e^+e^- and $p\bar{p}$ collider experiments are always arranged in such a way that the beams are colliding head-on with equal and opposite momenta. The CM frame is the natural reference frame for the data analysis of such collider experiments. The 3-momentum of Z^0 in the CM frame is zero ($\mathbf{q} = 0$) so that Z^0 is at rest in this frame. Additionally the center-of-mass frames of the in and out states are also at rest because $\mathbf{q} = 0$. Since all the relevant systems are at rest in the CM and lab frames, it is reasonable to expect that the widths at the Z^0 pole measured by collider experiments agree with the non-relativistic Breit-Wigner formula. In neutrino weapon applications, it is seldom practical to shoot the $\nu\bar{\nu}$ beams head-on. In the lab frame where the $\nu\bar{\nu}$ beams are colliding at oblique angles, the momenta of center-of-mass of $\nu\bar{\nu}$, Z^0 and $f\bar{f}$ are non-zero, $\mathbf{q} = \mathbf{p}_1 + \mathbf{p}_2 = \mathbf{p}_3 + \mathbf{p}_4 \neq 0$. In order to understand the phenomenology of the Z^0 pole in the $\mathbf{q} \neq 0$ case, the focus is directed to the type of collisions in that a resonance is moving relativistically with respect to the target. According to Eq. (16), the Z^0 pole is possible in a stationary target when the beam energy reaches 4×10^6 GeV for a positron beam on an electron target or 2×10^3 GeV for an anti-proton beam on a proton target. Such experiments do not exist. In the lower energy regime, nuclear physics experiments often shoot electron or photon beams at stationary targets. The resonances are usually excitations of proton so that the target and the resonance are at rest with respect to each other. In rare high energy reactions $e^+e^- \rightarrow Z^0 Z^0$ [20–23] and $p\bar{p} \rightarrow Z^0 Z^0$ [24], the condition $\mathbf{q} \neq 0$ is obtained automatically by virtue of integrating over \mathbf{p}_3 and \mathbf{p}_4 in the calculation of the cross section formula. However Z^0 is the out-state in this case and not the propagator so that the Breit-Wigner formula does not apply. To the best of the author's knowledge, there is no scattering experiment that satisfies the condition of $\mathbf{q} \neq 0$ at the Z^0 pole at the time of the writing of this paper.

At the Z^0 pole, most of the energy of the in-state is converted to the Z^0 mass so that the residual kinetic energy is relatively small. The Z^0 propagator is approximately at rest in the lab frame even though its momentum is non-zero $\mathbf{q} \neq 0$. Electron and neutrino, on the other hand, have very small mass so that a relatively small amount of transfer momentum \mathbf{q} will cause them to move relativistically. Z^0 is a virtual particle. Its influence is limited to a short time between the in and out states. As far as the in and out states in their center-of-mass rest frames are concerned, a moving Z^0 of total width Γ is effectively the same as a hypothetical stationary Z^0 of width Γ/γ . The advantage of modeling the propagator as a stationary Z^0 in the center-of-mass rest frame of the in-state is that this condition satisfies the assumption of the non-relativistic Breit-Wigner formula in that both the target and resonance are at rest with respect to each other. The similar argument can be repeated for the out-state. Following the same reasoning of Eq. (22), the propagator in the case of $\mathbf{q} \neq 0$ is taken to be

$$\frac{1}{(q^2 - M_Z^2 + 2im\Gamma)}, \quad (23)$$

where $m \in \{m_\nu, m_f\}$. The factor of 2 in the width term $im\Gamma$ of Eq. (23) comes from the fact that there are 2 particles of mass m in the in and out state. The subtlety of Eq. (22) is that the argument is crafted first in a preferred reference frame (such as the lab frame) and then generalized to be frame independent. Eq. (23) exploits the same strategy by incorporating a Lorentz factor $\gamma = q_0/(2m)$ in the center-of-mass rest frame of the in-state (out-state). q_0 as in $q = (q_0, \mathbf{q})$ is canceled from Eq. (23) by the factor $1/(2q_0)$. With Eq. (23), $\langle \mathcal{M}_Z^2 \rangle$ for $\mathbf{q} \neq 0$ can be re-evaluated by averaging the invariant amplitude squares computed with the new total widths corresponding to the in and out

states,

$$\begin{aligned} \langle M_Z^2 \rangle &\propto \frac{1}{2} \lim_{m_\nu \rightarrow 0} \left\{ \frac{1}{(q^2 - M_Z^2)^2 + 4m_\nu^2 \Gamma^2} + \frac{1}{(q^2 - M_Z^2)^2 + 4m_f^2 \Gamma^2} \right\} \\ &\simeq \frac{1}{2} \left\{ \frac{1}{(q^2 - M_Z^2)^2} \right\}. \end{aligned} \quad (24)$$

The last step of Eq. (24) is motivated by $1/m_\nu^2 \ll 1/m_f^2$. A third term constructed from the rest frame of Z^0 is not needed because it is redundant. In actuality, m_ν is small but non-zero. Assuming that $m_\nu \sim 0.1$ eV, $M_Z^4/m_\nu^2 \Gamma^2 \sim 10^{27}$. Instead of an infinite cross section as claimed earlier, the reaction rate at the Z^0 pole is only 27 orders of magnitude larger than that of the inverse beta decay. The improvement is adequate to make the idea of a neutrino counter nuclear weapon practical with reasonably intense $\nu\bar{\nu}$ beams. Therefore the invariant amplitude square in Eq. (15) is a good approximation up to a factor of 2.

III. SIMULATION RESULTS

The exact details of the designs of thermonuclear weapons are classified. However the basic principles of the operation of various types of nuclear weapon are unclassified and freely available through public information [25]. Generally speaking, a modern nuclear weapon is made up of a fission bomb (the primary stage) and a fusion bomb (the secondary stage). The primary stage typically has a plutonium core surrounded by a tamper, a neutron reflector and a set of chemical explosive lenses on the outermost layer. The tamper slows down the explosion just enough to increase the efficiency of the chain reactions. The neutron reflector increases the criticality of the fissile so that the efficiency of the explosion is further increased. In some designs (such as the W87 warhead), the tamper and neutron reflector seem to be combined in one layer made of beryllium. The secondary stage is a spherical or cylindrical complex of solid lithium deuteride (fusion fuel) interlaced with layers of uranium walls and the so-called ‘‘spark plug’’ in the center. A spark plug is a fissile lining that enhances compression. The sequence of explosions begins with the simultaneous ignition of the chemical explosive lenses in the primary stage to compress the sub-critical plutonium core to reach super-criticality by implosion. The heat and pressure generated by the fission bomb in the primary stage compress the fusion fuel in the secondary stage. Neutrons from the fission bomb convert the lithium-6 isotopes in solid lithium deuteride into tritium (${}^6_3\text{Li} + n \rightarrow {}^4_2\text{He} + {}^3_1\text{H} + 4.8$ MeV). Tritium and deuterium fuse to create a hydrogen bomb explosion. In a thermonuclear weapon, most of the energy is generated by fusion in the secondary stage. A sketch of the W87 warhead found online [26] is the source of the geometry used in the simulations of this work. More detailed discussions of thermonuclear weapon designs can be found on the same archive [27].

Neutrinos cannot be shielded and can reach a nuclear weapon anywhere on earth or in space as long as the location is specified and if the neutrino weapon can focus the high energy $\nu\bar{\nu}$ beams on the target accurately. High energy radiations produced by $\nu\bar{\nu}$ annihilation cause neutron spallation inside the fissile material that in turn initiate fission reactions. Fissions create heat. When heat is generated in sufficient quantity, it ignites the chemical explosive lenses surrounding the plutonium core in the primary stage of the thermonuclear warhead. This way $\nu\bar{\nu}$ annihilation provides a means to detonate a nuclear weapon remotely. The critical question is whether these annihilation-induced radiations can be generated efficiently and cheaply to make the idea practical. To this end, the simulation tool MCNPX2.5.0 is used to calculate the heat deposition by fissions from high energy external sources at $E_f = 45$ GeV, approximately half the value of M_Z . MCNPX2.5.0 is an integration between MCNP4B and LAHET2.8. It uses a very old version of FLUKA (FLUKA87) as a hadron generator above the INC (intranuclear cascade) region ($E > 10$ GeV). The manual of MCNPX2.5.0 explicitly states that it does not include any nuclear reactions for muon. Muon-induced neutron spallation has been observed experimentally and is already included in the more recent versions of FLUKA. A newer version of FLUKA is planned to be integrated in the next release of MCNPX so that this problem will hopefully be fixed in due time. Another problem of MCNPX2.5.0 inherited from LAHET is that not all particle types can be used as primaries. So far it is found that MCNPX will crash when τ is used as a primary. During the course of this work, it is also discovered that MCNPX has a strange bug when π^0 is used as a primary. The bug is already reported to the MCNPX team. In principle, spallation neutrons induced by μ^\pm , τ and π^0 can be simulated by the latest version of FLUKA and then input into MCNPX to calculate the fission deposition energy. Unfortunately the license agreement of FLUKA restricts the software to non-weapon-related use. Since the purpose of the present work is merely a feasibility study and not a detailed weapon design, the absence of μ^\pm , τ and π^0 as primaries in the simulations will not affect the conclusion. The remaining particle types used as primaries are e^\pm , π^\pm , K^\pm , K_L and K_S . Of course neutrinos can also be annihilation products. But they will not be a useful source of weapon related radiations and will not be simulated. Despite of the shortcomings aforementioned, the advantages of MCNPX are a complete set of nuclear libraries, very good neutron

simulations and a card to calculate fission energy deposition. Therefore MCNPX is still the best simulation tool for the purpose of the present study. In the absence of detailed designs of nuclear weapons and a complete simulation package, the present feasibility study is meant to be an order of magnitude estimation of fission energy deposition from annihilation-induced products.

The geometry of the primary stage of the W87 thermonuclear warhead used in the MCNPX simulations is illustrated in Fig. 3. Due to the spherical symmetry of the geometry, a uniform disk source is adequate to simulate random radiations on the core. On a 2 GHz Core Duo 2 processor, a particle history of an external e^\pm takes 2-3 hours to complete on one core. Primaries of other particle types may take only 2-3 minutes to finish. In order to be fair in the comparisons of all particle types, the same number of particle history (NPS) is used for all of the simulations, namely $NPS = 100$. Table II summarizes the annihilation-induced fission energy deposition on the plutonium core of a mocked-up W87 warhead. The unit of fission energy deposition output by MCNPX is MeV/g/p (where p stands for ‘‘primary’’) and is converted to MeV/p by multiplying the output with the mass of the plutonium core 1.0015×10^4 g. The energy deposition on the human body is simulated by shooting the primaries from a point source inside a rectangular parallelepiped of $200 \times 100 \times 100$ cm³ made with a material of similar chemical composition of the human body as shown in Table III. The simulation results of annihilation-induced energy deposition on the human body is summarized in Table IV. The unit of energy deposition in MCNPX is MeV/g/p and is converted to Gray per primary (Gy/p) where Gray is defined as J/Kg. The large errors in Tables II and IV are partly due to varying slant depths when the primaries intersect different parts of the targets.

A typical accelerator such as MINOS can produce neutrinos (93% ν_μ , 6% $\bar{\nu}_\mu$ and 1% $\nu_e + \bar{\nu}_e$) from a beamline of 2×10^{13} protons/s. High energy protons interact in a target on the NUMI beamline to produce pions and kaons, which decay into muons and muon neutrinos ($\pi^+ \rightarrow \mu^+ \nu_\mu$). Muons further decay into electrons and neutrons ($\mu^+ \rightarrow e^+ \nu_e \bar{\nu}_\mu$). The energy spectrum peaks at approximately 3 GeV with a long high-energy tail extending to 120 GeV [28]. Assuming a hypothetical situation in that the peak of the neutrino spectrum is tuned to $M_Z/2$ for the Z^0 pole, much of energy is still lost to smearing and the production of by-products. An accelerator of the size of Fermilab is not practical for neutrino weapon applications because of the problem of maneuverability and the prohibitive cost. According to Table II, the typical fission energy deposition is in the 10^4 MeV/p range. Assuming a very optimistic estimate of 5% efficiency for energy transfer, neutrinos produced by an optimized version of MINOS and its antineutrino counterpart will create enough annihilation-induced radiations to convert the plutonium core in Figure 3 into a 1–10 kW reactor. Suppose that the chemical explosive around the plutonium core is C4 which is 91% RDX (cyclotrimethylene-trinitramine) and has a flash point at 234°. Reference [1] estimates the heat capacity of ^{239}Pu as 6.557×10^{11} MeV/g·K while Reference [29] shows a more detailed temperature dependent heat capacity profile for both pure and alloyed plutonium as 30–40 J/mol·K at 20–250 °C. As an approximation, this work takes the heat capacities of the plutonium alloy and beryllium to be 8×10^{11} MeV/g·K and 1.14×10^{13} MeV/g·K respectively. A MINOS-induced 1–10 kW heater can detonate a plutonium core in Figure 3 in 100–1000 seconds. Long heating time will likely lead to the heating of the area surrounding the plutonium core. Before the temperature in the primary stage reaches the flash point of the explosive, the polyethylene filler may melt and the supporting structure may expand. If the position of the fissile shifts relative to its surrounding, the effectiveness of the explosive lenses may be affected in such a way that a fizzle (not a full scale nuclear explosion) occurs. In case the nuclear weapon is moving, it is tactically advantageous to minimize the heating time because of the technical difficulty of tracking. For these reasons, the heating time should be limited to approximately 1 s to detonation. The main disadvantage of a conventional accelerator is not just the long heating time but also its size and cost. Fortunately recent breakthroughs on tabletop accelerators may one-day be the solution for all these problems. Plasma accelerators utilizing the laser-driven Wakefield can achieve an electric field gradient up to 270 GeV/m depending on the electron density in the plasma. The electron beam produced by Laser Wakefield Acceleration (LWFA) is stable and collimated [30]. LWFA has some potential limitations. A study shows that electric field breakdown occurs at 13.8 ± 0.7 GeV/m in some dielectric [31]. In one report, a mono-energetic electron beam up to 1 GeV driven by a 40 TW laser in a 3.3 cm-long hydrogen-filled capillary discharge wave guide has been successfully demonstrated [32]. The peak current achieved is up to 300 A (2×10^{21} electrons/s). At the time of the writing of this paper, the highest peak current published by another report is 100 pC/10 fs or 10 kA [33, 34]. Results of a positron laser-plasma accelerator is recently published [35] so that all of the essential components for the construction of $\nu\bar{\nu}$ beams are already in place. Assuming a typical femtosecond laser pulse rate of 30 kHz at the current level of technology, LWFA $\nu\bar{\nu}$ beams of 1–10% efficiency for energy transfer can detonate the plutonium core in Figure 3 in 50–500 s.

The radiations produced by the neutrino counter nuclear weapon can also irradiate human beings. The lethal dose for a typical human adult is 10-20 Grays. According to Table IV, the dosage from annihilation-induced radiations is in the $10^{-14} - 10^{-12}$ Gy/p range. Assuming an average dosage of 10^{-13} Gy/p per beam and the same parameters of the LWFA $\nu\bar{\nu}$ beams above, a neutrino tactical weapon takes 10–100 s to achieve the lethal dose per person.

IV. ENGINEERING

Neutrino beams are typically produced by colliding particles on suitable targets in a high energy accelerator such as those in MINOS and CNGS to create pions and kaons which decay into neutrinos, small amount of anti-neutrino and hadrons. As it is shown above, a Fermilab size accelerator is not practical for the purpose of a neutrino counter nuclear weapon because a counter weapon has to be small, mobile and must have aiming capability. Laser wakefield accelerator (LWA) is small and agile. It has already succeeded in producing 1 GeV electrons in a space of less than 1 cm long so that it has potential to be the accelerator of choice for a neutrino counter nuclear weapon. In LWA, an intense laser femtosecond laser pulse creates a bubble of ion cavity that follows the laser pulse. Electrons create a wakefield in the ion cavity which in turn accelerate other electrons. MCNP simulation shows that each neutrino anti-neutrino annihilation at the Z_0 pole deposits about 104 MeV of energy on the plutonium core. Taking into consideration the heat capacity of plutonium and the temperature of the flash point of the explosive surrounding the plutonium core, a LWA based neutrino counter nuclear weapon operated on a 1 TW laser can in principle detonate a nuclear weapon in a few minutes. The next generation of femtosecond laser is projected to reach Peta Watts. It is possible to create a LWA based neutrino counter nuclear weapon that can detonate a nuclear warhead instantaneously.

Currently LWA makes an electron beam by accelerating electrons through the ion bubble in a plasma. A positron beam is made by an entirely different technique which uses a powerful laser to bombard a target (e.g. gold foil) to generate and accelerate positrons at the same time. When electron and positron beams hit suitable targets to create pions and kaons, they decay into neutrinos and anti-neutrinos in similar ways as those in MINOS and CNGS. This conventional method of generating neutrino and anti-neutrino beams is not very energy efficient. In MINOS and CNGS, a 120 GeV proton beam produces 12-14 GeV neutrinos. The mass of Z_0 is about 91G eV. Depending on the angle θ between the neutrino and anti-neutrino beams the transfer momentum square is $q^2 \simeq 2E_\nu E_{\bar{\nu}}(1 - \cos\theta)$ according to Eq. (16). It can be seen that the neutrino and anti-neutrino beam energies need to be comparable to the Z_0 mass. Using conventional method to generate neutrino and anti-neutrino beams, the LWA electron and positron beam energies have to be in the order of 1 TeV. Assuming an accelerating gradient of 1 GeV/cm for LWA, the length of the accelerator must be more than 100 m which is beginning to challenge the assumption that a LWA based neutrino counter nuclear weapon is compact. Additionally pion and kaon decays do not produce pure neutrino and anti-neutrino beams. Mixture of neutrino species in a beam adds to the complexity of engineering design. Therefore a non-conventional technique for generating neutrino and anti-neutrino beams is needed.

CERN has been experimenting with the idea of beta beam which involves accelerating heavy ions that are beta emitters [36]. Low Q value neutrino and anti-neutrino emitters are ${}^6\text{He}$ and ${}^{18}\text{Ne}$. High Q value emitters such ${}^8\text{Li}$ and ${}^8\text{B}$ can provide neutrinos and anti-neutrinos at 3.5 times the energies compared to low Q value emitters. For a Lorentz factor of $\gamma = 100$, the neutrino and anti-neutrino beta beams generated so far can reach the energy range of atmospheric neutrinos (2 TeV to 200 TeV) which is more than adequate to create a Z_0 pole. Currently beta beam is made by conventional RF accelerators. Research has been conducted on using LWA to accelerate heavy ions for more than a decade [37]. Currently Trident Laser Facility at LANL has achieved 100 MeV to 1 GeV proton and heavy ion energy through laser-driven acceleration by hitting a suitable target with a table top laser [38]. However beta emitters may not be accelerated using the laser bombardment technique. Instead it is hoped that technology may soon allow the integration of LWA and beta beam for neutrino counter nuclear weapon applications.

Some of the key challenges of a LWA based neutrino counter nuclear weapon are plasma instability and neutrino beam quality. Plasma instability in LWA is being actively researched [39]. Physicists are now using LWA to build x-ray lasers so that confidence on the LWA beam quality is reasonable [40]. In the conventional colliders such as Tevatron and LHC, the proton and anti-proton beams are squeezed just before the collision to increase the particle density and hence collision probability. In a neutrino counter nuclear weapon, squeezing neutrino and anti-neutrino beams prior to the neutrino anti-neutrino annihilation is not a possibility. Therefore the neutrino and anti-neutrino beams have to be produced very collimated and dense from the start to increase of probability of collisions. The beam energies also need to be very fine tuned to improve the efficiency of neutrino anti-neutrino annihilation at the Z_0 pole. Therefore many technological problems still need to be solved before a LWA beta beam based neutrino counter nuclear weapon is feasible.

V. DISCUSSIONS AND CONCLUSION

An order of magnitude calculation based on a mocked-up design of the W87 warhead and a set of preliminary MCNPX simulations shows that radiations from $\nu\bar{\nu} \rightarrow f\bar{f}$ reactions at the Z^0 pole is capable of detonating a nuclear weapon remotely. The theory of the neutrino weapon capitalizes on the large cross section of the Z^0 pole at oblique angles. If the assumptions of relativistic arguments leading up to Eq. (24) are incorrect and that the width is not substantially reduced as claimed, the efficiency of a neutrino weapon will seriously suffer to the point of being

impractical. Assuming that the theory is correct, the efficiency of the neutrino weapon will largely depend on our ability to control the parameters in Eq. (16) to satisfy the condition $q^2 = M_Z^2$ exactly. Since $\langle \mathcal{M}_Z^2 \rangle \sim 1/[q^2 - M_Z^2]^2$ in Eq. (15), an agreement between E_ν and $E_{\bar{\nu}}$ with M_Z to 4 significant figures implies a 10^{12} increase in the cross section and so on. In reality, there will always be a smear of neutrino energy around the Z^0 pole. Too much smearing will decrease the efficiency of the neutrino weapon. The reaction $\nu\bar{\nu} \rightarrow \nu\bar{\nu}$ also decreases the efficiency of the neutrino weapon but this effect is predictable and inconsequential. The heat transfer from the plutonium core to the chemical explosives can in principle be reduced by thermal insulation or by changing the design to a gun-type trigger mechanism. These fixes will most likely reduce the efficiency of a nuclear weapon and may not protect the weapon from being detonated remotely. The neutrino counter nuclear weapon can also be used as a tactical weapon. The advantage of a neutrino tactical assault weapon is that it can hit hard-to-reach places such as deep underground concrete bunkers and caves in mountainous areas. Since neutrinos can travel across the globe in the speed of light, a neutrino weapon does not allow the time for an early warning system. Since neutrinos cannot be shielded, a neutrino weapon is in principle non-defensible. A preliminary analysis of the capability of a neutrino weapon given above is based on the experimental designs of plasma accelerators. The order of magnitude estimates show that the current level of technology is already meeting the minimum hardware requirements. It is foreseeable that high quality and high intensity e^+e^- beams will be made available by LWFA and similar technologies soon. The remaining technological challenge is to engineer collimated mono-energetic high intensity $\nu\bar{\nu}$ beams using beta emitters. Accelerator R&D will be the most critical part of the development of a neutrino weapon. Experimental verification of the near-singularity of the Z^0 pole at oblique angles is also very important. Since neutrino propagation through the Earth is affected by neutrino oscillation and matter effect, basic neutrino physics research is needed to measure the physical parameters accurately. In order to obtain maximal collision efficiency, the $\nu\bar{\nu}$ beams must be focused on a small spatial region. Due to the relatively low rate of lethal radiation on a human body, a neutrino tactical weapon is a unlikely candidate for a weapon of mass destruction. At the end, it is hoped that the neutrino counter nuclear weapon will make nuclear weapons obsolete so that the goal of non-proliferation is achieved peacefully.

Acknowledgments

The author thanks the Chinese University of Hong Kong for hosting his visit during the period of this research. V. Taranenko, G. W. McKinney, M. Sher, W. M. Morse, W. Simmons and C. G. R. Geddes have graciously provided helpful criticisms and discussions that improve the quality of the paper at various stages.

-
- [1] H. Sugawara, H. Hagura and T. Sanami, hep-ph/0305062.
 - [2] F. Suekane, Nuclear Physics B (Proc. Suppl.) **235-236** (2013), 33-38.
 - [3] B. L. Young, "Current status of neutrino physics", 34(2): Chinese Physics C **34** (2010), 287-298,
 - [4] D. Griffiths, "Introduction to Elementary Particles", Wiley, New York (1987).
 - [5] P. D. B. Collins, A. D. Martin and E. J. Squires, "Particle Physics and Cosmology", Wiley, New York, 1989.
 - [6] S. Weinberg, "The Quantum Theory of Field I", Cambridge, Cambridge, 1995.
 - [7] W.-M. Yao *et al.*, Review of Particle Phys G **33**, 1 (2006).
 - [8] M. E. Peskin and D. V. Schroeder, "An Introduction to Quantum Field Theory", Westview Press, Boulder, CO, 1995.
 - [9] P. Kielanowski, quant-ph/0312178 (21 December 2003).
 - [10] M. Nowakowski and A. Pilaftsis, Z. Phys. C **60**:121-126 (1993); hep-ph/9305321.
 - [11] S. De Leo and P. Rotelli, JETP Lett. **76**, 56-60 (2002), hep-ph/0109014.
 - [12] R. J. Crewther, J. Finjord and P. Minkowski, Nuclear Phys B **207**, 269-287 (1982).
 - [13] F. Abe *et al.* (CDF Collaboration), Phys. Rev. Lett. **77**:2616-2621 (1996).
 - [14] L. D. Landau and E. M. Lifshitz, "Quantum Mechanics: Non-relativistic theory", Pergamon, Oxford, 1977.
 - [15] D. M. Manley, Phys. Rev. D **51**:4837-4843 (1995).
 - [16] E. V. Balandina, E. M. Leikin and N. P. Yudin, nucl-th/030601.
 - [17] B. Krusche *et al.*, Phys. Rev. Lett. **74**:3736-3739 (1995). B. Krusche *et al.*, Phys. Rev. Lett. **75**:3023 (1995).
 - [18] M. Dugger *et al.* (CLAS Collaboration), Phys. Rev. Lett. **89**:222002 (2002).
 - [19] F. Renard *et al.* (GRAAL Collaboration), Phys. Lett. B **528**:215-220 (2002).
 - [20] R. Barato *et al.* (ALEPH Collaboration), Phys. Lett. B **469**:287-302 (1999).
 - [21] J. Abdallah *et al.* (DELPHI Collaboration), Eur. Phys. J. C **30**:447-466 (2003).
 - [22] P. Achard *et al.* (L3 Collaboration), Phys. Lett. B **572**:133-144 (2003).
 - [23] G. Abbiendi *et al.* (OPAL Collaboration), Eur. Phys. J. C **32**:303-322 (2004).
 - [24] U. M. Abazov *et al.* (D0 Collaboration), Phys. Rev. D **78**:072002 (2008).
 - [25] J. Bernstein, "Nuclear Weapons: What You Need to Know", Cambridge, Cambridge (2008).

- [26] “The W87 Warhead”, Nuclear Weapon Archive, <http://nuclearweaponarchive.org/Usa/Weapons/W87.html>.
- [27] “Thermonuclear Weapon Designs”, Nuclear Weapon Archive, <http://nuclearweaponarchive.org/Nwfaq.Nfaq4-5.html>.
- [28] P. Adamson *et al.* (MINOS Collaboration), *Phys. Rev. D* **76**, 072005 (2007).
- [29] R. Gröper, “Heat capacity of pure and alloyed plutonium”, LA-UR-07-2534.
- [30] J. Faure, C. Rechatin, A. Norlin, A. Lifschitz, Y. Glinec and V. Malka, *Nature* **744**, 737 (7 December 2006).
- [31] M. C. Thompson *et al.*, *Phys. Rev. Lett.* **100**, 214801 (2008).
- [32] A. J. Gonsalves *et al.*, “GeV Electron Beams from a Centimeter-scale laser-driven Plasma Accelerator”, Proceedings of PAC07, Albuquerque, NM, 25-29 June 2007, 1911-1915.
- [33] C. B. Schroeder, W. M. Fawley, E. Esarey and W. P. Leemans, “Design of an XUV FEL driven by the laser-plasma accelerator at the LBNL LOASIS facility”, Proceedings of FEL 2006, Bessy, Berlin, Germany.
- [34] J. van Tilborg *et al.*, *Phys. Rev. Lett.* **96**:014801 (2006).
- [35] X. Wang *et al.*, *Phys. Rev. Lett.* **101**:124801 (2008).
- [36] E. Wildner, “Beta Beam for Neutrino Production”, *Nuclear Physics B (Proc. Suppl.)* **00** (2010), 1-5.
- [37] Ito Hiroaki, Bakhtiari Mohammad, Imai Masashi, Yugami Noboru and Nishida Yasushi, “Ion Acceleration in Laser Wakefield”, *J. Plasma Fusion Res. Series*, **4** (2001), 335-339.
- [38] Daniel Jung, “Ion Acceleration from Relativistic Laser Nano-target Interaction”, Ph. D. dissertation for Fakultät für Physik of Ludwig Maximilians Universität (München 2012).
- [39] C. M. Huntington, A. G. R. Thomas, C. McGuffey, T. Matsuoka, V. Chvykov, G. Kalintchenko, S. Kneip, Z. Najmudin, C. Palmer, V. Yanovsky, A. Maksimchuk, R. P. Drake, T. Katsouleas, and K. Krushelnick, “Current Filamentation Instability in Laser Wakefield Accelerators”, *PRL* **106**, 105001 (2011).
- [40] S. Corde, K. Ta Phuoc, G. Lambert, R. Fitour, V. Malka, A. Rousse, A. Beck and E. Lefebvre, “Femtosecond X Rays from Laser-plasma Accelerators”, *Reviews of Modern Physics*, **85** (January-March 2013), 1-48.

Figures

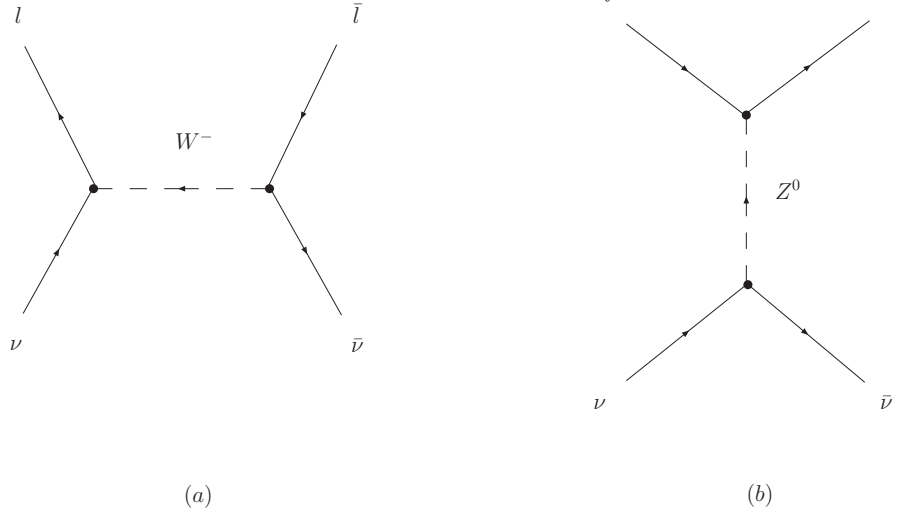


FIG. 1: Tree-level Feynman diagrams of neutrino-antineutrino ($\nu\bar{\nu}$) annihilation with (a) a charged current and (b) a neutral current. The products of $\nu\bar{\nu}$ annihilation is a lepton-antilepton pair ($l\bar{l}$) in the charge current case and a fermion-antifermion pair ($f\bar{f}$) in the neutral current case. The fermion f can be a lepton, neutrino or quark. In the case of quark production, mesons will be created by hadronization.

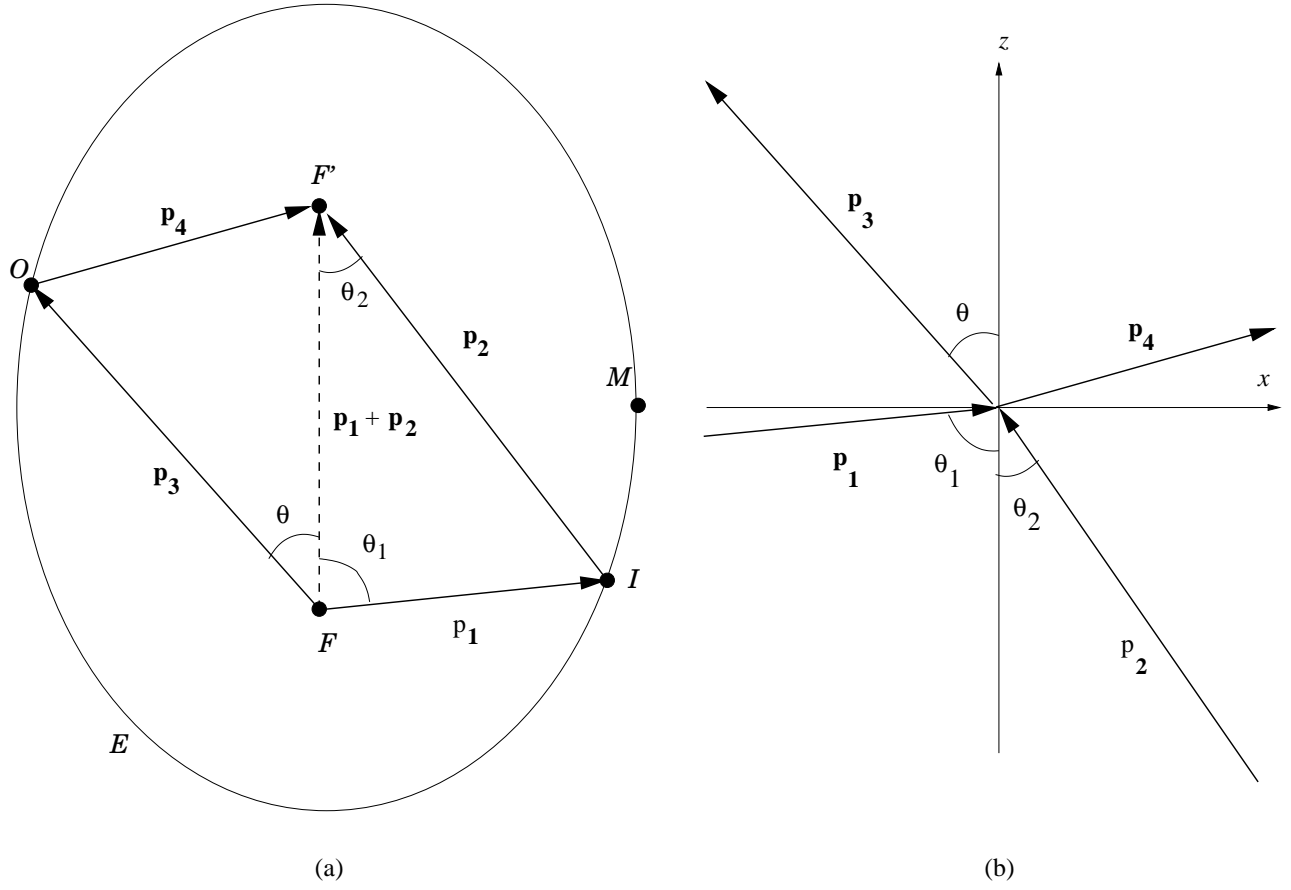


FIG. 2: Graphical representation of incoming 3-momenta \mathbf{p}_1 and \mathbf{p}_2 and outgoing 3-momenta \mathbf{p}_3 and \mathbf{p}_4 . The point \mathcal{O} lies on the ellipsoid \mathcal{E} in part (a) of the figure. The point \mathcal{I} is fixed by the incoming 3-momenta. Part (a) shows a special case in which all the 3-momenta lie on the same plain. \mathcal{F} and \mathcal{F}' are the foci of the ellipsoid. The point \mathcal{M} lies on the minor axis of \mathcal{E} . If $\mathcal{M} = \mathcal{I}$, $\theta_1 = \theta_2$. Momentum is conserved on \mathcal{E} , namely $p_1 + p_2 = p_3 + p_4$. Part (b) illustrates the Cartesian coordinates used to define the set of 3-momenta.

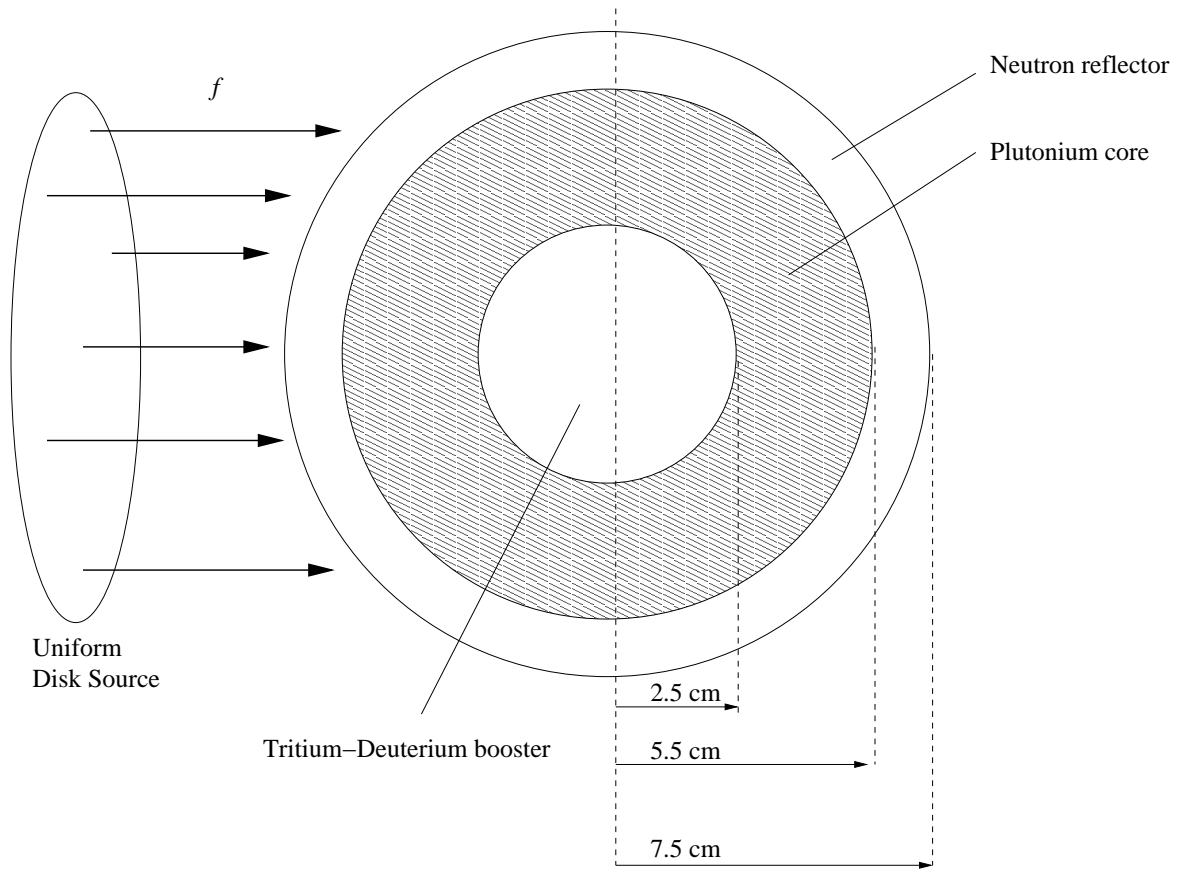


FIG. 3: A mock-up of the primary stage of the W87 thermonuclear warhead with the explosive lenses removed. The core is made out of plutonium alloy (99.4% ^{239}Pu and 0.6% natural gallium). The density of plutonium alloy is 15.86 g/cc. The neutron reflector is made of beryllium. The density of Be is 1.85 g/cc. The tritium-deuterium booster has a density of 0.00175 g/cc. The source is $f \in \{e^\pm, \pi^\pm, K^\pm, K_L, K_S\}$.

Tables

TABLE I: Neutral vector and axial vector couplings in the GWS Model [4].

f	C_V	C_A
ν_e, ν_μ, ν_τ	$\frac{1}{2}$	$\frac{1}{2}$
e^-, μ^-, τ^-	$-\frac{1}{2} + 2 \sin \theta_w$	$-\frac{1}{2}$
u, c, t	$\frac{1}{2} - \frac{4}{3} \sin \theta_w$	$\frac{1}{2}$
d, s, b	$-\frac{1}{2} + \frac{2}{3} \sin \theta_w$	$-\frac{1}{2}$

TABLE II: Fission energy deposition E_c from $\nu\bar{\nu}$ annihilation-induced products used as primaries p on the plutonium core of the primary stage of a mocked-up W87 thermonuclear warhead. The geometry is illustrated in Fig. 3. The number of particle history is 100. The energy of the primaries is $E_f = 45$ GeV.

p	E_c (10^4 MeV/ p)
e^\pm	2.30 ± 0.36
π^\pm	5.80 ± 0.59
K^\pm	2.59 ± 0.39
K_L	2.11 ± 0.34
K_S	1.58 ± 0.25

TABLE III: Approximate chemical composition of the human body. The average mass and density of a human body is taken to be 75 Kg and 1.4 g/cc respectively.

Element	Relative Atomic Composition
O	65
C	18
H	10
N	3
Ca	1.5
P	1.2
K	0.2
S	0.2
Cl	0.2
Na	0.1
Mg	0.05

TABLE IV: Energy deposition E_h from $\nu\bar{\nu}$ annihilation-induced products used as primaries p on the human body. The chemical composition of the human body is given in Table III. The number of particle history is 100. The energy of the primaries is $E_f = 45$ GeV.

p	E_h (Gy/ p)
e^\pm	$(2.22 \pm 0.10) \times 10^{-12}$
π^\pm	$(5.03 \pm 0.63) \times 10^{-14}$
K^\pm	$(4.06 \pm 2.07) \times 10^{-14}$
K_L	$(3.62 \pm 1.03) \times 10^{-14}$
K_S	$(3.39 \pm 0.96) \times 10^{-14}$